

The Onera *elsA* CFD software: input from research and feedback from industry

LAURENT CAMBIER^a, SÉBASTIEN HEIB AND SYLVIE PLOT

Onera – The French Aerospace Lab, 92322 Châtillon, France

Received 31 January 2013, Accepted 11 April 2013

Abstract – The Onera *elsA* CFD software is both a software package capitalizing the innovative results of research over time and a multi-purpose tool for applied CFD and multi-physics. The research input from Onera and other laboratories and the feedback from aeronautical industry users allow enhancement of its capabilities and continuous improvement. The paper presents recent accomplishments of varying complexity from research and industry for a wide range of aerospace applications: aircraft, helicopters, turbomachinery...

Key words: Navier-Stokes / aerodynamics / aircraft / helicopter / turbomachinery

1 Introduction

For about 15 years at Onera, the *elsA* software is simultaneously a basis for Computational Fluid Dynamics (CFD) research, a software package capitalizing on the innovative results of research over time, a tool allowing investigation and understanding of flow physics, and a multi-purpose tool for applied CFD and multi-physics [1–5]. The range of aerospace applications covered by *elsA* is very wide [6]: aircraft, helicopters, tilt-rotors, turbomachinery, counter-rotating open rotors (CROR), missiles, unmanned aerial vehicles (UAV), launchers. . .

As a matter of fact, the aerodynamic analysis and design in aerospace today require high levels of accuracy and reliability which result from studies in several domains: physical modelling, numerical methods, software engineering, efficiency on rapidly evolving hardware and extensive validation by comparison with experimental databases. The capitalization of various research results in the *elsA* multi-purpose code allows in the first place the sharing of common CFD features for simulating external flows around airframes or internal flows in turbomachinery. In the second place, it allows the selection over the wide range of capabilities, of the features which are best suited to the application, since there is no universal CFD method answering all of the problems.

The research studies, software development and validation activities, dealing with *elsA*, rely on a project approach necessary to cope with the complexity of today's CFD. This project approach is coordinated by Onera and

involves input from other research laboratories and feedback from aeronautical industry. The objective of the paper is to show recent outstanding accomplishments both from the research side and from the industry side.

2 General description of *elsA*

First, let us briefly recall the main features of the *elsA* software (see a more detailed overview in [5]). The *elsA* multi-application CFD simulation platform deals with internal and external aerodynamics from the low subsonic to the high supersonic flow regime and relies on the solving of the compressible 3-D Navier-Stokes equations. *elsA* allows the simulation of the flow around moving deformable bodies in absolute or relative frames. A large variety of turbulence models from eddy viscosity to full differential Reynolds stress models (DRSM) are implemented in *elsA* for the Reynolds averaged Navier-Stokes (RANS) equations [7, 8]. Laminar-turbulent transition modelling relies either on criteria, or on solving additional transport equations [7]. Various approaches for Detached Eddy Simulations (DES) [9, 10] and Large Eddy Simulations (LES) are also available.

Complex geometrical configurations may be handled using high flexibility techniques involving multi-block structured body-fitted meshes: these techniques include patched grid and overset capabilities (Chimera technique [11, 12]). From this initial multi-block structured meshing paradigm, *elsA* is presently evolving toward a quite complete multiple-gridding paradigm including the local use of unstructured grids [13–15] in some blocks of

^a Corresponding author: Laurent.Cambier@onera.fr

a multi-block configuration as well as adaptive Cartesian grids [11, 12].

The system of equations is solved by a cell centered finite-volume method. Space discretization schemes include classical second order centered or upwind schemes and higher order schemes. The mostly used integration of the semi-discrete equations relies on a backward Euler technique with implicit schemes solved by robust LU relaxation methods. The convergence is accelerated by the use of multigrid techniques for steady flows. The implicit Dual Time Stepping (DTS) method or the Gear scheme is employed for time accurate computations.

elsA also includes an “aeroelasticity module” [16, 17] offering a framework for aeroelastic simulations and an “optimization module” for calculation of sensitivities by linearized equation solution or by adjoint solver techniques [18, 19].

elsA is based on an Object-Oriented (OO) design method and is coded in three programming languages: C++ as main language for implementing the OO design, Fortran for CPU efficiency of calculation loops, Python for the user interface. A good CPU and parallel efficiency is reached on a large panel of computer platforms.

3 Research partners and industry users

The development and the validation of the *elsA* software benefit by inputs from research partners and feedback from industry users. By first considering the research side, the Cerfacs organization (Toulouse) is an important *elsA* partner since 2001 and has been participating over the last decade to research studies and software development dealing in particular with mesh strategies [13], numerical methods [20–24] and CPU efficiency [25]. Other main research partners are the Fluid Mechanics and Acoustics lab (LMFA, École Centrale de Lyon) [26] and Cenaero (Belgium) [27] for turbomachinery flow simulation, and the Dynfluid lab (Arts et Métiers ParisTech) for high accuracy numerical schemes [28, 29] (see Sect. 5 for activities about *elsA* by Cerfacs, LMFA, Cenaero and Dynfluid). The Von Karman Institute also uses *elsA* for turbomachinery flow simulation (see the validation study of the transport equation transition model in Ref. [30]).

Whereas it is rather unusual for a CFD software package to deal both with external flows around aircrafts or helicopters and with internal flows in turbomachinery, *elsA* is today used as a reliable tool by Airbus for transport aircraft configurations, by Safran group for turbomachinery flow simulations and by Eurocopter for helicopter applications (see Sect. 4). Among other users, let us mention MBDA for missile configurations and Électricité de France for steam turbine applications [31].

A two-day workshop gathering simultaneously research partners and industry users is organized every two years to share experience. The results presented in the paper either are issued from the last *elsA* workshop, or correspond to more recent accomplishments. We will

present some real-world applications from the main industry users. Then, we will show results from Onera and research partners, mostly illustrating prospects for future use.

4 Results from industry users

This section presents some examples of the use of *elsA* by three of our main industry partners: Safran, Airbus and Eurocopter.

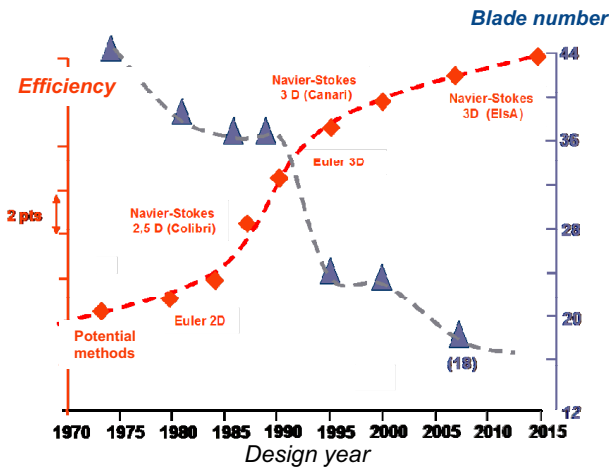
4.1 Turbomachinery results

Figure 1 provided by Snecma company (Safran group) shows some *elsA* results for modern fans. The two curves illustrate the contribution of the Onera CFD software (*elsA* in recent years) to the simultaneous progress of the efficiency of the conventional fans (more than 10 points in 30 years) and the reduction of the blade number (twice less blades). Examples of simulations are shown for a conventional fan, a counter rotating fan and a CROR.

The *elsA* software has been strongly validated by Onera and Safran for various turbomachinery configurations and is today intensively used for design studies which rely for a part on isolated row simulations, and for the major part on multi-stage applications. Best practice on space and time numerical schemes, turbulence and transition modelling, boundary conditions have been defined through comparisons with experiment and with legacy code results. The design work includes studies on technological effects, such as rotating and non-axisymmetrical platforms, mass flow injection or suction, casing treatments, grooves, cooling holes.

Figure 2 shows a typical result of flow simulations performed by Snecma on a multi-stage configuration. The approximate steady flow calculations through multi-stage machines are today usual in design process. In *elsA*, they rely on a specific steady condition based on azimuthal averages, the mixing plane condition, to connect two consecutive rows. This type of simulation gives a quite good prediction of the overall efficiency of a machine, even if of course it does not give any information on the flow unsteadiness, as may be given by the more costly Reduced Blade Count technique and Phase-Lagged (or chorochronic) method also available in *elsA* for time-periodic flows [5].

The number of mesh points for the 4-stage low pressure turbine configuration of Figure 2 is about 10 million. Numerical settings for the steady flow simulation are the following: second order Jameson scheme, backward Euler implicit time integration scheme, LU-SSOR implicit technique, multigrid convergence acceleration. Turbulence modelling relies on Wilcox (k, ω) model. Converged solution is obtained on Snecma computer in less than one day. Figure 2 presents the flow field in the complete 8-row computational domain. Numerical results show a good comparison with measured static pressure on the vane walls. The comparison of the isentropic Mach



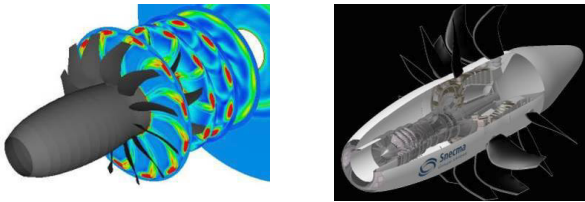
(a) Evolution over time of efficiency and blade number



Modern fan with 18 blades



Counter rotating fan with 10 + 14 blades



Counter rotating open rotor with 12 + 10 blades

(b) Results of *elsA* simulations carried out by Snecma

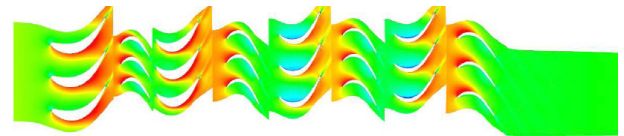
Fig. 1. Contribution of CFD to improvement of efficiency (courtesy of Safran/Snecma).

number on one of the distributors for different span locations (here shown at mid-span) is also satisfactory.

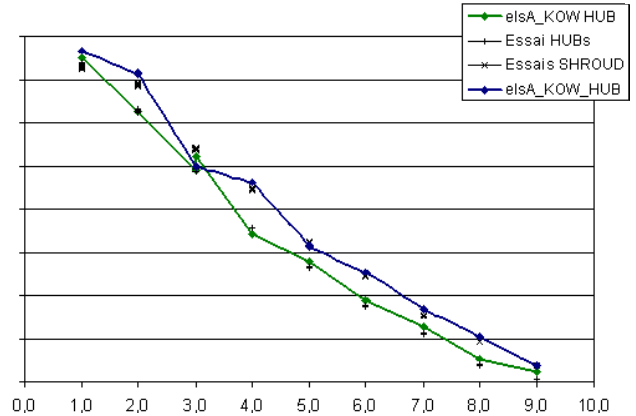
elsA software is also used by other turbomachinery manufacturers of the Safran group: Turbomeca for helicopter engines and Techspace Aero for fans and boosters.

4.2 Transport aircraft results

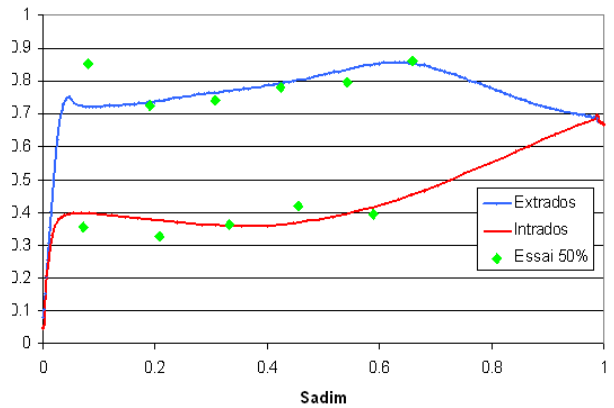
CFD based on Navier-Stokes equations has today reached a maturity level in terms of accuracy, robustness and efficiency, which makes it essential for the daily work



(a) Iso-absolute Mach number at mid-span



(b) Wall static pressure ($\Delta p = 2000$ Pa) on the hub and on the shroud : comparison with experiment



(c) Isentropic Mach number on the wall of a distributor (mid-span): comparison with experiment.

Fig. 2. Snecma results with *elsA* on a 4-stage turbine (courtesy of Safran/Snecma).

of aerodynamic engineers of transport aircraft manufacturers. Navier-Stokes CFD has been introduced for many years in Aerodynamic Design and Data processes of Airbus with the following objectives:

- quickly deliver more optimized aircraft components aerodynamic shapes;
- evaluate Reynolds effects, jet effects, ground effects by extrapolating results known on an existing aircraft;
- prepare, analyse and, if necessary, correct wind tunnel and flight tests.

Airbus today uses *elsA* as its structured multi-block tool with various join types and Chimera overset grids. There has been a massive ramp-up of the use of Chimera technique in daily production during the last few years. Thanks to this technique, control surface applications

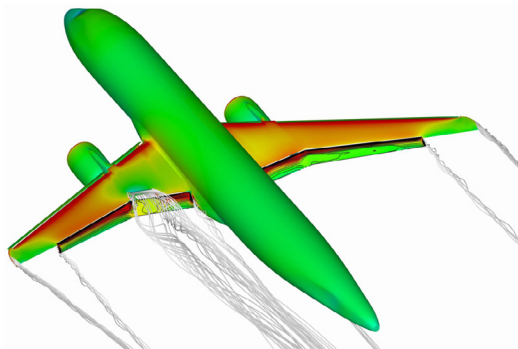


Fig. 3. Pressure coefficient calculated by *elsA* for a generic aircraft in landing configuration with/without internal spoiler deployed (Onera calculation).

are now commonly realized with structured meshes. This overset technique also gives to Airbus plenty of opportunities to apply it in an easy and fast turnaround manner: antenna on fuselage, wing tip effect, Vortex generators...

Figure 3 proposed by Airbus shows the pressure coefficient field for a twin wing-mounted turbofan generic transport aircraft in landing configuration. Two calculations carried out by the Applied Aerodynamics Department at Onera are represented on this unique figure: without deployment of the internal spoiler on the right, and with deployment of the spoiler on the left. The multi-block mesh includes more than 140 blocks and more than 33 million mesh points for the deployed configuration. This type of configuration is considered as very difficult to calculate with block-structured meshes. Thanks to the use of Cassiopée pre-processing tools [11, 32] delivered with the *elsA* software suite, these calculations illustrate the possibilities of the Chimera technique to deal with such configurations. These results are considered by Airbus of utmost importance for performance prediction of the landing configurations.

Thanks to *elsA* Chimera features, Airbus is also able to simulate the unsteady flow in a representative shape of the landing gear cavity of a transport aircraft (Fig. 4). A first mesh is defined for the basic configuration including four Chimera domains respectively for the cavity, for the fuselage, for the wheel and pylon and for a triangle added plate. Then, to study the influence of an internal spoiler, which was proposed in order to reduce the rear door loads, a second Chimera mesh is defined by adding to the first mesh an internal spoiler Chimera domain. The second computation shows a high rear door load reduction by putting an internal spoiler at the middle of the cavity. The conclusion of Airbus on this type of simulation is positive on the ability of the Chimera strategy to deal with complex landing gear configurations and to quickly test additional element effect, as well as on the *elsA* features for simulating unsteady flows.

Another *elsA* feature appreciated by Airbus is the full adjoint for optimum design. Figure 5 shows a pilot optimization application done in full reverse mode. For a wing geometry parametrisation based on 179 variables,

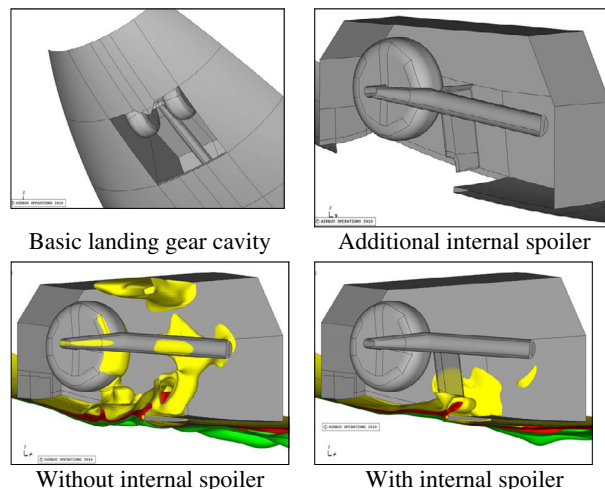


Fig. 4. Landing gear cavity unsteady simulation – Effect of an internal spoiler – Iso-Mach contours (*green*: $M = 0.2$; *red*: $M = 0.15$; *yellow*: $M = 0.1$) at a given time (courtesy of Airbus).

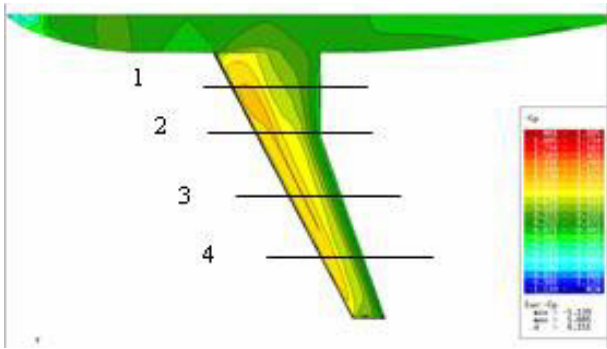
the drag optimization with lift kept constant allows a drag reduction of about 3 drag counts. Figure 5 shows the evolution of the pressure coefficient distributions in 4 sections for the initial and optimized wings.

4.3 Helicopter results

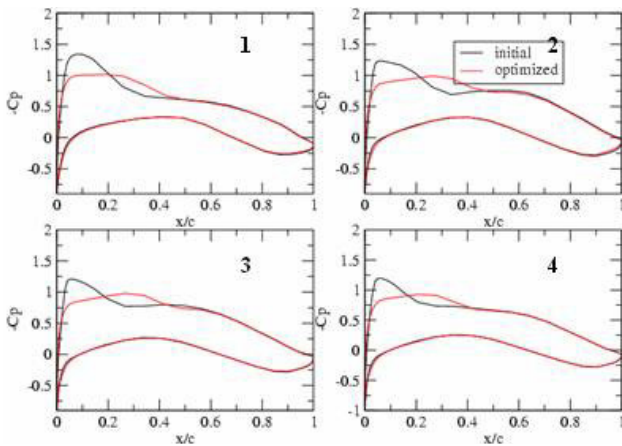
CFD simulation around helicopters is today possible with a detailed representation of the geometry which includes the rotor head with complete mechanism. One important objective of such simulation is to establish a drag breakdown of the rotor head, element by element, in order to determine the most important contributors to the total drag. Moreover, the effect of taking into account rotor head rotation in the CFD simulation is determined as shown in Figure 6.

Besides, this type of simulation is used for studying the tailshake phenomenon which corresponds to a modal excitation of the structure of the rear parts of the helicopter (tail beam, tail plane, fin) by the wake of the upper parts of the helicopter (rotor head, chimney, engine cowling). This type of study requires a good prediction, not only of the aerodynamic field around the rotor head, but also of the wake location and conservation. Figure 7 shows the result of an unsteady *elsA* simulation carried out by Eurocopter in a 36 million point mesh on 85 processors. A second order in space numerical scheme is used. The turbulence model is the Wilcox (k, ω) model with the SST correction.

The drag prediction and the tailshake simulation both require high quality matchings between Chimera blocks, a fine mesh in the region of the rotor head wake and high quality numerics. Whereas the *elsA* simulation today provides with an accurate drag prediction, further improvement, such as the use of higher order schemes and interpolations, is necessary for a deeper understanding of the tailshake physics.



(a) Iso-contours of the pressure coefficient on the optimized wing



(b) Evolution of the C_p distributions in sections 1 to 4 between initial wing and optimized wing

Fig. 5. Pilot optimization application with *elsA* in full reverse mode (courtesy of Airbus).

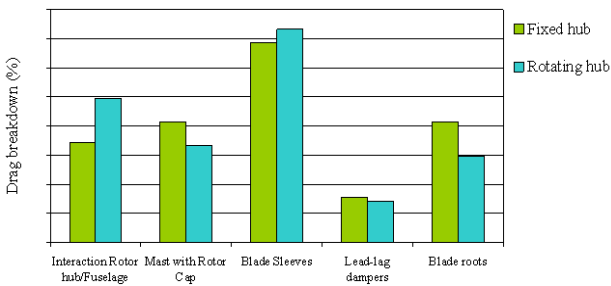


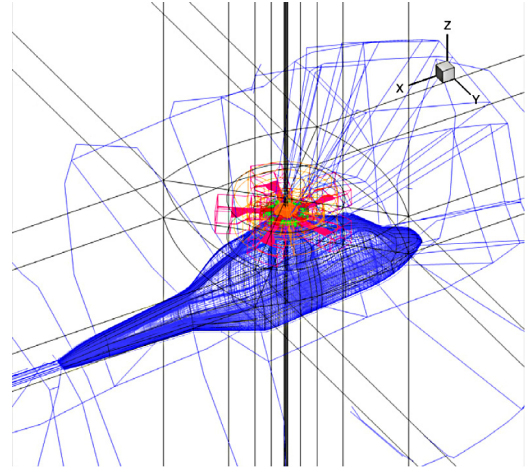
Fig. 6. Drag breakdown given by an *elsA* simulation (courtesy of Eurocopter).

5 Results from Onera and research partners

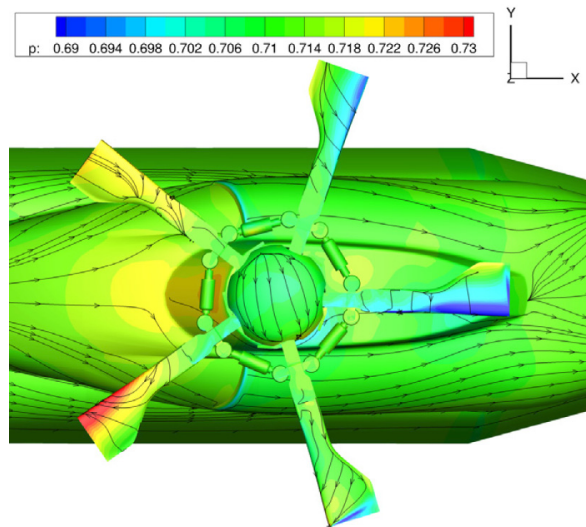
This section presents results from Onera and research partners in order to highlight advanced features on turbulence modelling, mesh strategies, numerics and aeroelasticity.

5.1 Modelling for turbulent flows

Whereas most of the design studies are done with a few one- or two-equation turbulence models



(a) Mesh of the helicopter with complete rotor head



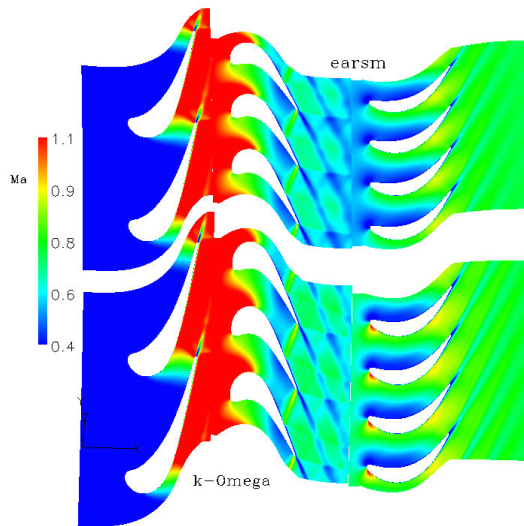
(b) Pressure isocontours and friction lines on the walls

Fig. 7. *elsA* simulation around an helicopter with complete rotor head (courtesy of Eurocopter).

(Spalart-Allmaras model, (k, ω) and (k, ε) families, (k, l) Smith model), more advanced turbulence models for RANS equations are studied and developed in *elsA* [7], such as the non-eddy viscosity EARSM (explicit algebraic Reynolds stress) [8] and DRSM models. In order to deal with flows exhibiting strong unsteadiness and large separated regions, LES, RANS/LES and DES [9, 10] techniques are also an important *elsA* research topic. We present in this section two results of these advanced modelling techniques.

5.1.1 EARSM turbulence modelling for a turbine flow simulation (LMFA work)

This section presents the result of a simulation carried out by LMFA (see Ref. [26] for another *elsA* simulation by LMFA for a car turbocharger compressor).



(a) Iso-absolute Mach number at mid-span

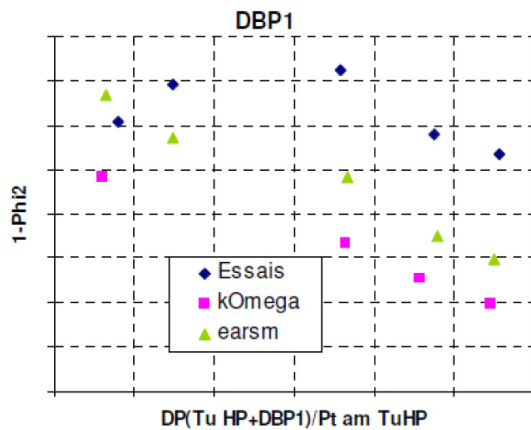
(b) Losses in the low pressure distributor ($\Delta x = \Delta y = 2\%$)

Fig. 8. *elsA* simulation in a turbine: comparison between (k , ω) and EARSM (courtesy of LMFA and Snecma).

The configuration provided by Snecma is composed of a high pressure turbine stage followed by the first row of the low pressure turbine. Simulations with the (k , ω) model predict too small losses on the low pressure distributor, in comparison with the experiment. The objective of the study of LMFA was to evaluate if a more advanced turbulence model would offer a better prediction. The considered turbulence model has been implemented in *elsA* by the Department of Modelling in Aerodynamics and Energetics (DMAE) at Onera. It is an EARSM model [8] based on the (k , kl) two-equation model proposed a few years ago by DMAE. The turbulence closure is no more based on the Boussinesq assumption as for the basic (k , kl) model, but on a non-linear relation between the Reynolds tensor and the mean velocity gradients through the Wallin-Johansson expression of the anisotropy tensor [33].

Figure 8a shows a comparison of the flow fields obtained by the (k , ω) model (below) and the EARSM

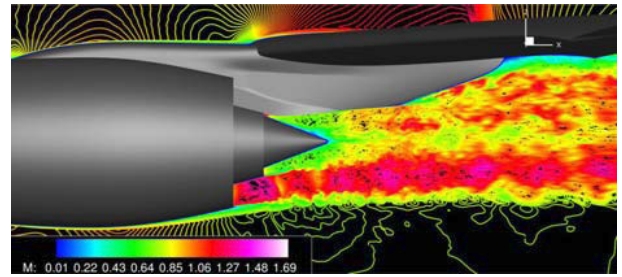


Fig. 9. ZDES *elsA* simulation with the RFG technique: instantaneous Mach field at mid-span on the JEDI configuration (Onera simulation from [34]).

model (above). On the prediction of losses (Fig. 8b), the comparison with experiment shows an improvement with the EARSM model. There is still an under-estimation of the losses, which may be attributed to the unsteady rotor-stator interaction effects, which were not taken into account in the steady simulation.

5.1.2 Simulation of a jet with Zonal DES (Onera work)

The DES-type approaches aim at combining the accuracy and low cost of the RANS model for attached boundary layers with the accuracy of the LES in separated regions and far from walls. These approaches are well adapted to installed double flux engine configurations since they allow for a deep analysis of turbulent structures inside mixing layers and of the interaction between the pylon wake and the jet. The flow simulation presented here and detailed in [34] corresponds to a wall-to-wall swept wing configuration equipped with a pylon and an air supply stick, and studied in transonic flow conditions in the S3Ch wind tunnel of Onera Meudon. The modelling [34] relies upon evolutions of the Zonal DES approach [9,10] and upon a turbulent Random Flow Generation (RFG) technique [35]. This RFG technique intends to represent the important turbulence levels which come from engines and which have a strong influence on the jet development. The grid is composed of about 175 million cells, mostly concentrated into the jet development region thanks to the patched-grid technique. Numerics is ordinary: second order in space centered scheme, second order in time Gear scheme with Newton sub-iterations, implicit LU-SSOR technique in each sub-iteration.

The computed instantaneous Mach flow field at mid-span (Fig. 9) shows the correct development of the shear layers as well as the complex interaction region between the pylon and the jets. Figure 10 presents a comparison with the experimental averaged velocity fields of the results of two ZDES simulations with and without turbulence generation inside the engine. The simulation with the RFG technique is in a better agreement with experiment, but some discrepancies remain, mostly because of the still too low injected turbulence. Results on velocity fluctuations [34] confirm the importance of a correct estimation of the turbulence rate of jets.

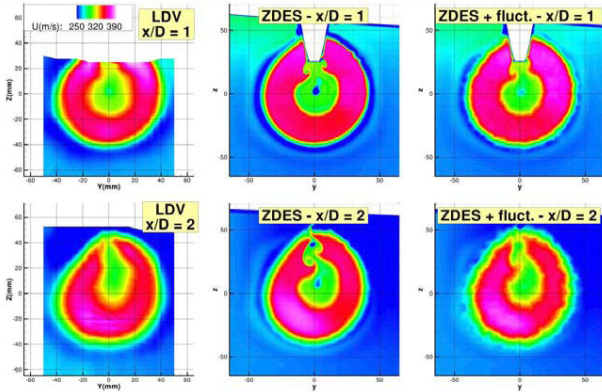


Fig. 10. Averaged velocity fields at $x/D = 1$ and 2. Left: LDV measurements – Middle: ZDES without RFG – Right: ZDES with RFG (Onera [34]).

5.2 Mesh strategies

Results presented in Section 4 show the complexity of the configurations (landing gear cavity, helicopter rotor head, turbomachinery technological effects) which may be handled with overset multi-block structured body-fitted meshes. Nevertheless, it is very useful to have the capability of using locally unstructured meshes in some of the blocks where it would become too difficult to build a structured grid. Besides, structured Cartesian grid capabilities are well adapted to high order spatial discretization and mesh adaptation, which in turn allows for better capturing of off-body flow phenomena such as shear layers and wakes. So, the objective of *elsA* is to progressively offer a quite complete multiple-gridding paradigm providing the potential for optimizing the gridding strategy on a local basis for each specific configuration. We present now two illustrations of this multiple-gridding evolution.

5.2.1 Hybrid solver (Onera/Cerfacs work)

Over the past few years, a cooperative work between Onera and Cerfacs [13–15] has allowed the extension of the multi-block structured solver in *elsA* to an hybrid grid solver, in which structured (ijk-based) and unstructured blocks may coexist within the same computational domain. Structured zones may be kept for the sake of efficiency and of accuracy in viscous layers, whereas unstructured zones may enable an easier mesh generation and adaptation process.

Development and validation of the hybrid features in *elsA* are still in progress, but the two following results show that the *elsA* hybrid capabilities already allow turbulent flow simulations in parallel, for both external and internal aerodynamics. Figure 11 shows the static pressure iso-contours given by the simulation of the 3D flow around the Onera M6 wing at $M_\infty = 0.84$ and $\alpha_\infty = 3.06^\circ$. The grid is composed of 32 unstructured blocks and the simulation is carried out on 32 processors. The Spalart-Allmaras turbulence model is used.

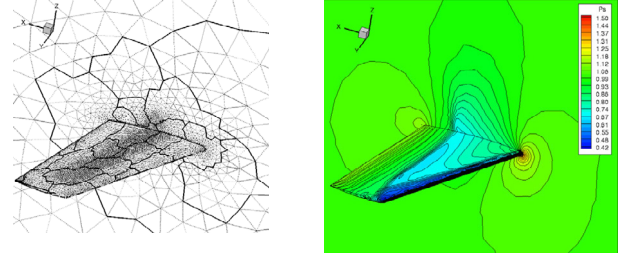


Fig. 11. *elsA* simulation of the M6 wing configuration: unstructured grid and static pressure iso-contours (Onera result from [15]).

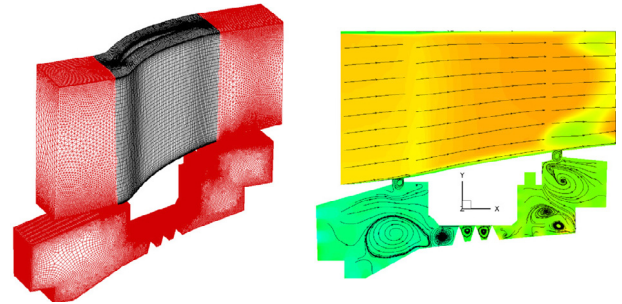


Fig. 12. *elsA* simulation in a shrouded stator : hybrid grid (unstructured blocks in red) and flowfield (streamlines in the cavity) (Onera result from [14]).

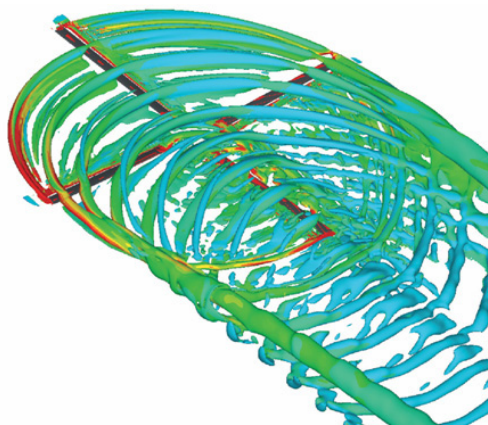
The second configuration corresponds to a shrouded stator. The hybrid grid remains structured around the blade and contains three additional unstructured blocks: two blocks located upstream and downstream of the blade and one block corresponding to the cavity underneath the hub. An unstructured grid generator is able to mesh the cavity by building only one block and in a shorter time than a multi-block structured generator. The Wilcox (k, ω) model is used.

5.2.2 Cartesian/curvilinear Chimera approach (Onera work)

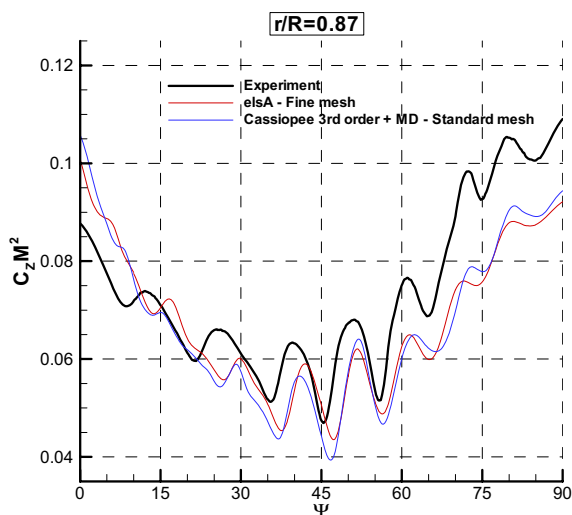
CFD progress allows an increased use of CFD for aeroacoustics. The Blade Vortex Interaction (BVI) noise, typical of helicopter applications, has been selected here to illustrate this topic. The challenge is to accurately capture the evolution of the blade tip vortex during the rotor revolution. The Chimera technique allows the overlapping of a curvilinear multi-block blade grid and Cartesian background grids.

Three grid resolution levels have been considered for inviscid unsteady simulations performed with second order scheme. In the finest mesh including 30 million cells, the wake is quite accurately captured with a strong vortex intensity kept during 1.5 revolutions (only during 0.5 revolution with the coarse grid), which is necessary for the interaction with the following blades (Fig. 13a).

The evolution of the sectional lift coefficient $C_z M^2$ at $r/R = 0.87$ on the advancing side (Fig. 13b) shows that the amplitude and the phase of all simulations are quite good with the finest mesh (no BVI oscillation is simulated



(a) Wake structure with the fine grid resolution



(b) Influence of mesh, adaptation and numerical scheme on airload fluctuations: advancing side BVI peaks

Fig. 13. *elsA* simulation for BO105 helicopter rotor in descent flight (Onera calculation from [6]).

by the coarse grid; see [6] for more details). When using a specific tool (Cassiopee Cartesian solver from Onera) which generates and automatically adapts these Cartesian grids, and in which a third order in space scheme is used, it is possible to obtain on a mesh of standard size (Fig. 13b) the same level of accuracy as that obtained on the fine mesh without adaptation and with second order scheme.

5.3 Numerics

Most of the *elsA* simulations are still done today by second order centered or upwind space numerical schemes. Nevertheless, the increasing needs for accuracy (for example, for aeroacoustics) and the objective of reducing the number of mesh cells for a given accuracy are strong incentives to study higher order schemes. Let us present two illustrations of this topic.

5.3.1 RBC schemes for the flow simulation in a turbine stage (Dynfluid/Onera work)

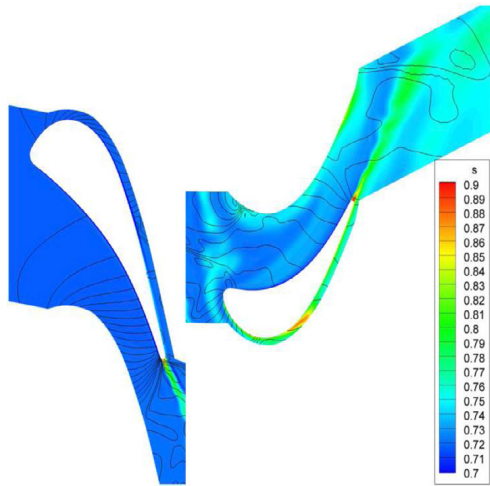
The Dynfluid lab in cooperation with Onera has been developing a class of numerical schemes called Residual-Based Compact (RBC) schemes [28,29]. Second and third order RBC schemes are available in *elsA*, whereas the study of fifth order RBC schemes is underway. The approximation is “compact” since it uses a stencil of only 3 points in each mesh direction. For general curvilinear grids, a weighted formulation (noted RBCi, “i” standing for “irregular”) ensures third order accuracy on mildly deformed mesh and at least second order accuracy on highly deformed meshes.

Figure 14 shows a comparison of the results obtained with the RBCi scheme with respect to those of the classical second order Jameson scheme (see Ref. [28] for more details). Quasi-3D unsteady computations are performed on a radial portion of the VKI BRITE HP transonic turbine stage. The use of chorochronic boundary conditions allows simulating just one blade per row. The RBCi scheme provides with a sharp capturing of shock waves and of von Karman vortices in the blade wakes, which are smoothed out by Jameson’s scheme.

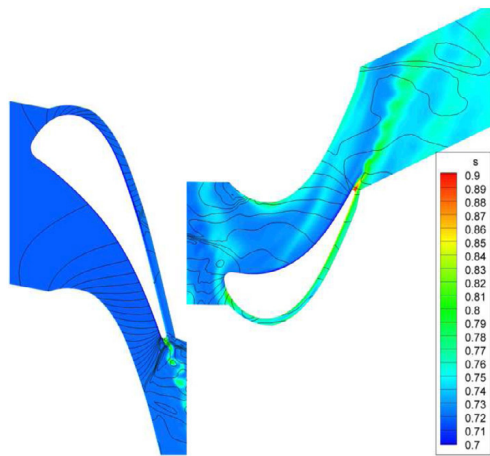
5.3.2 Jet noise simulation using high order LES (Cerfacs work)

The prediction of acoustics generated by a jet engine is a challenging task, due to the large disparity between the length and time scales of the flow field. To capture accurately such disparities, it is necessary to have numerical schemes that exhibit low dispersion and dissipation errors. Such schemes have been implemented in *elsA* [20]; they are based on a sixth order compact finite volume formulation. To ensure stability, a filtering operation (also based on a sixth order compact formulation) is necessary. The boundary conditions play a very important role for aeroacoustic computations, since acoustic waves reflecting on the boundary of the domain can completely pollute the simulation. Either non-reflecting Navier-Stokes Characteristic Boundary Conditions (NSCBC), or a radiation condition based on the asymptotic solution of the linearized Euler equations [21] are implemented to avoid such behaviour. An explicit Low Dissipation and Dispersion six stage Runge-Kutta scheme (LDDRK6) is used for time integration. The turbulence is taken into account via a LES approach where the subgrid-scale modelling is implicit, assuming that the energy transfer from large scales to small scales is provided by the filtering operation. The approach coupling LES for aeroacoustic sources and Ffowcs Williams – Hawkins analogy for acoustic propagation has been used. The classical ($M = 0.9$; $Re = 400\,000$) isothermal round jet has been simulated. The mesh includes about 20 million cells, which corresponds to a prediction up to a Strouhal number of 2.

The vorticity field (Fig. 15) shows the turbulent character of the flow at the exit nozzle, which results from



(a) Second order Jameson scheme



(b) Third order RBCi scheme

Fig. 14. Unsteady flow simulation in the VKI BRITE HP turbine stage (*elsA* result from [28]).

the vortex ring perturbation applied to the inlet boundary. The dilatation field (Fig. 15) perpendicular to the jet axis is a good indicator of the acoustic wave propagation.

The analysis of the overall sound pressure level (OASPL), which describes the contribution of all measured frequencies, shows that the noise directivity is accurately captured and the maximum error compared to experimental data is around 2 dB (Fig. 16).

5.4 Aeroelasticity

The “Ael” subsystem of *elsA* [16,17] developed by the Aeroelasticity and Structural Dynamics (DADS) Department of Onera gives access in a unified formulation to various types of aeroelastic simulations. The simulation types range from non-linear and linearized harmonic forced motion computations, to static coupling and consistent dynamic coupling simulations in the time-domain, with different levels of structural modelling (“reduced flexibility

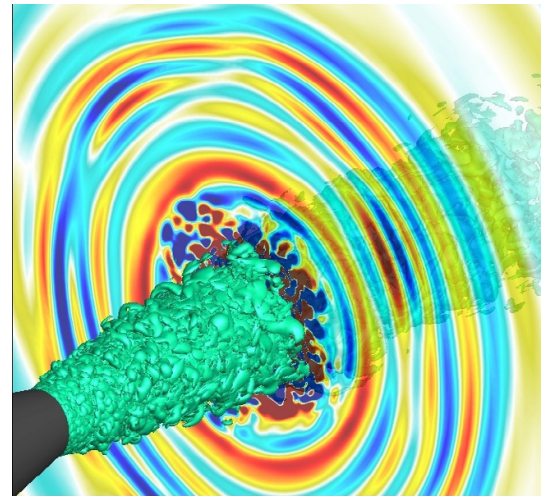


Fig. 15. Isothermal round jet LES *elsA* simulation: vorticity and dilatation fields (courtesy of Cerfacs).

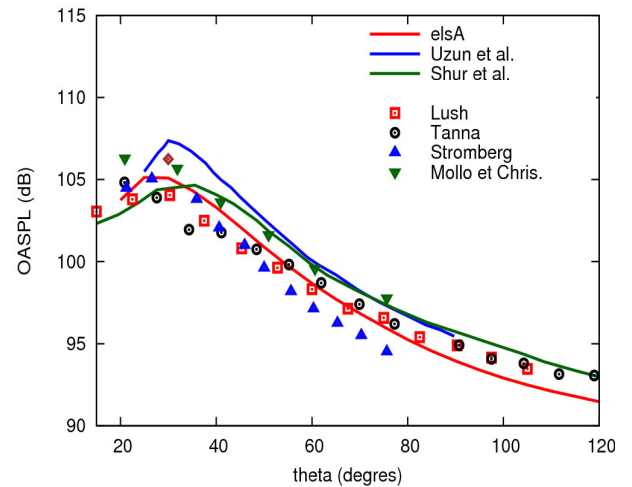


Fig. 16. Isothermal round jet simulation: spatial distribution of OASPL (courtesy of Cerfacs).

matrix” for static coupling, modal approach, or full finite element structural model).

5.4.1 Investigation of compressor blade vibrations due to subharmonic aerodynamic excitations (Cenaero work)

The first example of an aeroelastic simulation (see Ref. [27] for more details) deals with the forced response behaviour of a compressor blisk (resulting from the manufacturing of blades and disks as a single element). The one piece structure and the low weight of the blisk may lead to poor vibrational performance that is worth being known. The aeroelastic analysis is performed by computing the modal properties of the structure as well as the aerodynamical damping and forces acting on it.

The forced response behaviour due to a subharmonic Blade Passing Frequency Excitation is studied on a blisk of a low pressure compressor, designed at Techspace Aero.

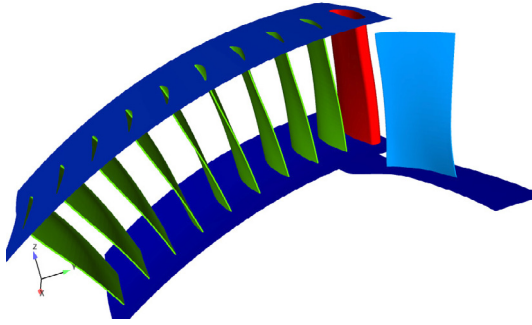


Fig. 17. Configuration to provide the 10 N excitation: one blade out of 10 stator blades is different (in red) (courtesy of Cenaero).

The related Campbell and ZZNF diagrams show crossing of the first bending mode with 10 engine orders (1 F/10 N). Since there are 100 stator blades upstream of the rotor, a practical solution to generate a subharmonic excitation (10 N) is to replace one out of 10 blades by a thicker one as presented in Figure 17.

The forced response is calculated in the following steps. First, with the assumption of the cyclic symmetry of the structure, only one sector is taken into account for the Finite Element modal analysis resulting from calculations with the Samcef code. Then, the aerodynamic damping is estimated by the unsteady RANS simulations performed with the *elsA* solver on a single rotor passage. The Smith (k, l) turbulence model is used. The time advancing is simulated by the DTS technique. Finally, the excitation force of 10 N is predicted by the *elsA* unsteady RANS computations with the chorochronic approach for the stage configuration shown in Figure 17.

One of the input parameters for the forced response estimation is the aerodynamic damping which is related to the flow unsteadiness generated by the blade dynamic motion. To measure the aerodynamic damping, the forced harmonic motion corresponding to the mode 1 F with constant amplitude is applied to the blade. This blade motion generates unsteady pressure which can either excite the structure or damp it. The analysis shows that the aerodynamic damping values for this test case are positive which help to avoid the flutter instabilities.

To evaluate the response of the mode 1 F, the excitation corresponding to the 10 N should be extracted. For this purpose, the calculated Generalized Aerodynamic Forces (GAF) are transferred to the frequency domain using Fast Fourier Transform. Figure 18 presents amplitude of the GAF versus the frequency. The part of the GAF which shows the impact of the thicker blade (10 N) and the part of all stator blades (100 N) is shown in the figure.

By taking into account only the excitation corresponding to the 10 N and solving the equation of motion of the structure, the forced response is estimated. Figure 19 presents the calculated amplification factor for a 10 N excitation. The comparison with the measurements reveals that the computations underestimate the forced response.

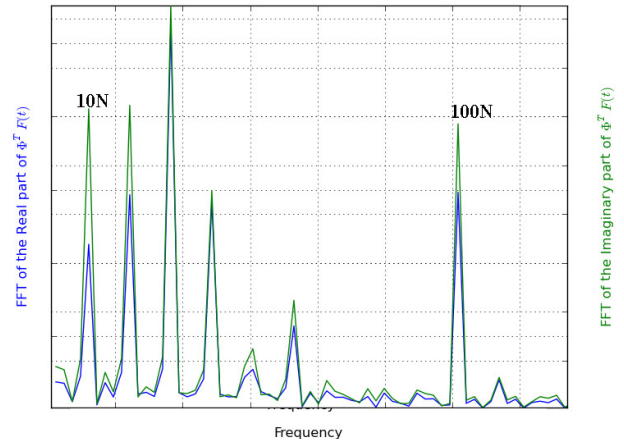


Fig. 18. GAF signal in frequency domain (courtesy of Cenaero).

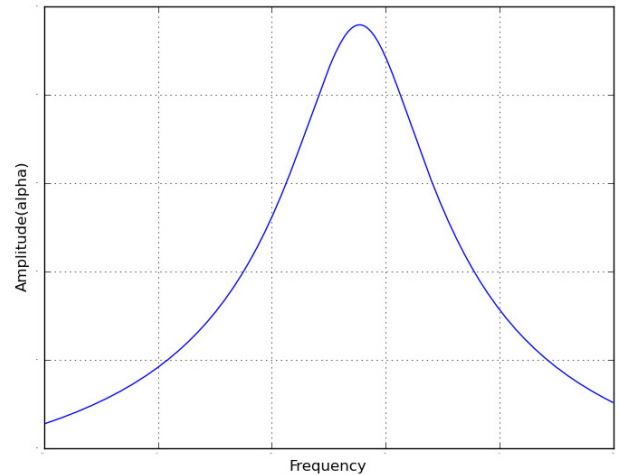


Fig. 19. Amplification factor vs. frequency for mode 1 F and excitation of 10 N (courtesy of Cenaero).

5.4.2 Dynamic forced response of a soft blade propeller due to incidence effect (Onera work)

The DADS Department of Onera is in charge of developing prediction capabilities concerning the aeroelastic behaviour of soft blade propellers and CRORs, in terms of flutter, whirl flutter and dynamic response, and also for evaluation of global loads [17]. Hereafter are presented some *elsA* results concerning the evaluation of the dynamic response of a soft blade model of the front propeller of a generic CROR configuration, due to an incidence effect.

The full 360° 11 blade generic propeller configuration (Fig. 20) is meshed, leading to a 121 structured block grid, including about 14 million cells. A view of the static pressure field computed by *elsA* on the rigid propeller at cruise conditions ($M_\infty = 0.73$ and $\alpha_\infty = 1^\circ$) is shown. In this case, due to incidence, the flowfield is unsteady, and produces a 1/rev periodic loading on each blade which is likely to induce periodic forced response of soft bladings, as shown below.

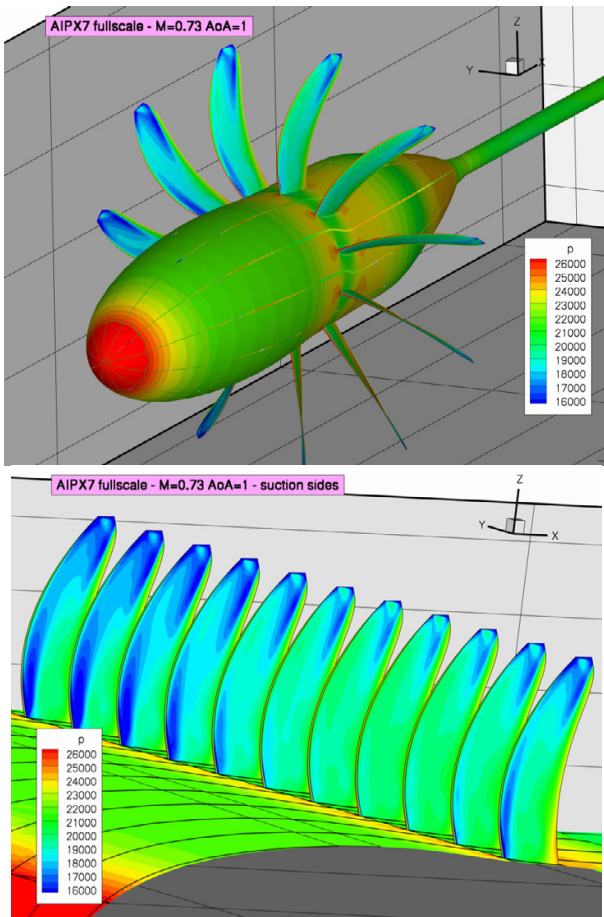


Fig. 20. Unsteady *elsA* simulation on a generic propeller rigid configuration (Onera simulation).

In a second step, after rigid blade computations, aeroelastic dynamic fluid-structure coupled computations have been carried out using the Ael aeroelasticity module of *elsA*, in order to study the forced response of the soft model, due to an incidence effect. A modal structural model has been implemented, including first and second bending and first torsion modes at nodal diameter 1, likely to be excited by the diameter 1 loading due to incidence.

During the transient computation, several pieces of information are collected: generalized coordinates and forces histories, global loads history such as thrust or vertical force. These data are post-processed in order to extract the frequency response in terms of blade deformation and forces: 1/rev forced response deformation and force levels are extracted, as well as aeroelastic modal dampings. Such an analysis, performed at the same cruise conditions, is presented in Figure 21. The 1/rev forced response peak is visible, as well as broader peaks at modal frequencies, illustrating damped modes.

Fluid-structure dynamic coupling simulations are conducted with *elsA/Ael* over 10 full propeller rotation cycles, using the Spalart-Allmaras turbulence model. The DTS scheme is used. Simulations are run in parallel on a Linux Xeon cluster using 44 processors, for about 5 days.

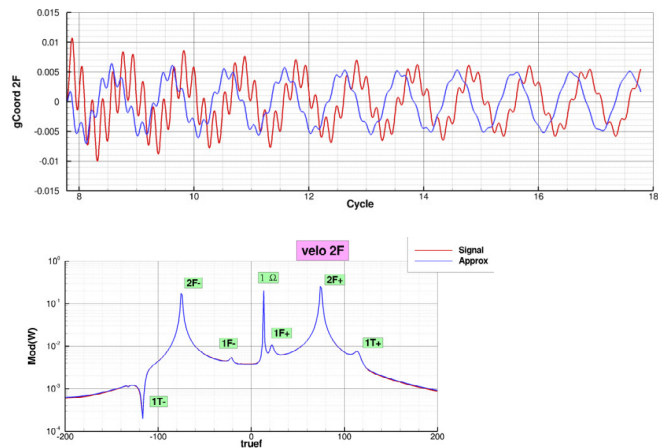


Fig. 21. Second bending response in time and frequency domains at 1° angle of attack (Onera simulation).

Investigations continue on this configuration, especially concerning the development of whirl flutter prediction capabilities for propellers as well as CROR models.

6 Concluding remarks

The wide range of applications both from industry users and from Onera and research labs shows that the *elsA* software has reached a high level of maturity, even if we were not able to show all the covered fields, such as CFD and wind tunnel synergy [36], car turbochargers [26], steam turbines [31], wind turbines, missiles, launchers. . .

Further improvements are still requested for satisfying the demand for better physical modelling (for the simulation of detached flows), for more accuracy (for example, for aeroacoustics), for more efficiency (to deal with the very fine meshes requested for simulating detached flows), for faster response times (for even more intensive use in design loops or optimization loops). The feedback of industry users on real-world configurations and the help of research partners to carry out the future enhancements are more than ever necessary to cope with all these challenges.

Acknowledgements. We want to acknowledge the following contributions to the paper: Snecma (Safran group) for Section 4.1, Airbus for Section 4.2, C. François (Onera) for the landing aircraft simulation, Eurocopter for Section 4.3, G. Ngo Boum (LMFA) for the EARSM turbine simulation, V. Brunet (Onera) for the ZDES jet simulation, M. de la Llave Plata and M.-C. Le Pape (Onera) for the simulations in hybrid grids, T. Renaud (Onera) for the Cartesian/curvilinear rotor simulation, B. Michel (Onera) and P. Cinnella (Dynfluid) for RBC results, H. Deniau (Cerfacs) for the high order LES jet noise simulation, F. Thirifay (Cenaero) for the blisk forced response and A. Dugeai (Onera) for the propeller forced response. Many thanks also to all those who have made *elsA* software project so successful for many years! This paper is a revised version of a paper entitled “The Onera *elsA* CFD software: input from research and feedback from industry” presented at the 28th International Congress of the Aeronautical Sciences, Brisbane, 23rd–28th September 2012.

Appendix

Over the years, *elsA* has been the basis for many studies by Onera and research partners which have been published in international journals. In addition to the 17 references [4–7, 11, 12, 16, 18–25, 28, 29] based on *elsA* in peer-reviewed journals, the following list (alphabetically by the first author) gathers nearly 100 other papers dealing with *elsA* in such journals. This list is again a demonstration of cooperative work about *elsA* since the co-authors often belong to several research labs, or to both research laboratories and industry.

- G. Alleon, S. Champagneux, G. Chevalier, L. Giraud, G. Sylvand, Parallel distributed numerical simulations in aeronautic applications, *J. Appl. Math. Model.* 30 (2006) 714–730
- P. Ardonneau, S. Trapier, Drag evolution of a rectangular wing with triggered wing-tip separation, *J. Aircraft* 42 (2005) 1369–1371
- C. Benoit, G. Jeanfaivre, Three-dimensional inviscid isolated rotor calculations using chimera and automatic cartesian partitioning methods, *J. Am. Helicopter Soc.* 48 (2003) 128–138
- A. Benyahia, R. Houdeville, Transition prediction in transonic turbine configurations using a correlation-based transport equation model, *Int. J. Eng. Syst. Model. Simul.* 3 (2011) 36–45
- F. Blanc, Patch assembly: An automated overlapping grid assembly strategy, *J. Aircraft* 47 (2010) 110–119
- F. Blanc, F.X. Roux, J.-C. Jouhaud, Harmonic balance-based code-coupling strategy for the calculation of aeroelastic system response to forced excitation, *AIAA J.* 48 (2010) 2472–2481
- S. Bocquet, P. Sagaut, J.-C. Jouhaud, A compressible wall model for Large-Eddy Simulation with application to prediction of aerothermal quantities, *Phys. Fluids* 24 (2012)
- T. Braconnier, M. Ferrier, J.-C. Jouhaud, M. Montagnac, P. Sagaut, Towards an adaptive POD/SVD surrogate model for aerodynamic design, *Comput. Fluids* 40 (2011) 195–209
- O. Brodersen, M. Rakowitz, S. Amant, P. Larrieu, D. Destarac, M. Sutcliffe, Airbus, ONERA, and DLR results from the second AIAA Drag Prediction Workshop, *J. Aircraft* 42 (2005) 932–940
- N. Buffaz, I. Trébinjac, Detailed analysis of the flow in the inducer of a transonic centrifugal compressor, *J. Thermal Science* 21 (2012) 1–12
- N. Bulot, I. Trébinjac, Impeller-diffuser interaction: analysis of the unsteady flow structures based on their direction of propagation, *J. Thermal Science* 16 (2007) 193–202
- N. Bulot, I. Trébinjac, Effect of the unsteadiness on the diffuser flow in a transonic compressor stage, *International Journal of Rotating Machinery* DOI:10.1155/2009/935293 (2009)
- N. Bulot, I. Trébinjac, X. Ottavy, P. Kulisa, G. Halter, B. Paoletti, P. Krikorian, Experimental and numerical investigation of the flow field in a high-pressure centrifugal compressor impeller surge, *J. Power Energy* 223 (2009) 657–666
- L. Castillon, G. Legras, Overset grid method for simulation of compressors with nonaxisymmetric casing treatment, *J. Propuls. Power* 29 (2013)
- J. Cliquet, R. Houdeville, D. Arnal, Application of laminar turbulent criteria in Navier-Stokes computations, *AIAA J.* 46 (2008) 1182–1190
- Y. Colin, H. Deniau, J.-F. Boussuge, A robust low speed preconditioning formulation for viscous flow computations, *Comput. Fluids* 47 (2011) 1–15
- E. Collado, N. Gourdain, F. Duchaine, L.Y.M. Gicquel, Effects of free-stream turbulence on high pressure turbine blade heat transfer predicted by structured and unstructured LES, *J. Heat Mass Transfer* 55 (2012) 5754–5768
- B. Courbet, C. Benoit, V. Couaillier, F. Haider, M.-C. Le Pape, S. Péron, Space Discretization methods, *Aerospace Lab* 2 (2011)
- N. Courtiade, X. Ottavy, N. Gourdain, Modal decomposition for the analysis of the rotor-stator interactions in multistage compressors, *J. Thermal Science* 21 (2012) 276–285
- D. Destarac, J. van der Vooren, Drag/thrust analysis of jet-propelled transonic transport aircraft; definition of physical drag components, *Aerosp. Sci. Technol.* 8 (2004) 545–556
- G. Dufour, F. Sicot, G. Puigt, C. Liauzun, A. Dugeai, Contrasting the harmonic balance and linearized methods for oscillating-flap simulations, *AIAA J.* 48 (2010) 788–797
- A. Dumont, A. Le Pape, J. Peter, S. Huberson, Aerodynamic shape optimization of hovering rotors using a discrete adjoint of the Reynolds-Averaged Navier-Stokes equations, *J. Am. Helicopter Soc.* 56 (2011) 032002
- F. Gand, V. Brunet, S. Deck, Experimental and numerical investigation of a wing-body junction flow, *AIAA J.* 50 (2012) 2711–2719
- F. Gand, Zonal Detached Eddy Simulation of a civil aircraft with a deflected spoiler, *AIAA J.* 51 (2013) 697–706
- E. Garnier, P.Y. Pamart, J. Dandois, P. Sagaut, Evaluation of the unsteady RANS capabilities for separated flows control, *Comput. Fluids*, 61 (2012) 39–45
- A. Giauque, B. Ortun, B. Rodriguez, B. Caruelle, Numerical error analysis with application to transonic propeller aeroacoustics, *Comput. Fluids*, 69 (2012) 20–34
- L.Y.M. Gicquel, N. Gourdain, J.-F. Boussuge, H. Deniau, G. Staffelbach, P. Wolf, T. Poinot, High performance parallel computing of flows in complex geometries, *C. R. Mécanique* 339 (2011) 104–124

- N. Gourdain, L.Y.M. Gicquel, G. Staffelbach, O. Vermorel, F. Duchaine, J.-F. Boussuge, T. Poinot, High performance parallel computing of flows in complex geometries – part 2: applications, *Comput. Sci. Discovery* 2 (2009) 1–28
- N. Gourdain, F. Leboeuf, Unsteady simulation of an axial compressor stage with casing and blade passive treatments, *J. Turbomach.* 131 (2009) 021013
- N. Gourdain, M. Montagnac, J.-F. Boussuge, Numerical Simulation of an axial compressor with non axisymmetric casing treatment, *Progress in Propulsion Physics* 1 (2009) 593–608
- N. Gourdain, S. Burguburu, F. Leboeuf, G. Michon, Simulation of rotating stall in a whole stage of an axial compressor, *Comput. Fluids* 39 (2010) 1644–1655
- N. Gourdain, M. Montagnac, F. Wlassow, M. Gazaix, High performance computing to simulate large scale industrial flows in multistage compressors, *Int. J. High Perform. Comput. Appl.* 24 (2010) 429–443
- N. Gourdain, L.Y.M. Gicquel, E. Collado, Comparison of RANS simulation and LES for prediction of wall heat transfer in a highly loaded turbine guide vane, *J. of Propuls. Power* 28 (2012) 423–433
- N. Gourdain, F. Wlassow, X. Ottavy, Effect of tip clearance dimensions and control of unsteady flows in a multi-stage high-pressure compressor, *J. Turbomach.* 134 (2012) 051005
- T. Guedeney, A. Gomar, F. Gallard, F. Sicot, G. Dufour, G. Puigt, Non-uniform time sampling for multiple-frequency harmonic balance computations, *J. Comput. Phys.* 236 (2013) 317–345
- J.-L. Hantrais-Gervois, A. Cartiéri, S. Mouton, J.-F. Piat, Empty wind tunnel flow field computations, *Int. J. Eng. Syst. Model. Simul.* 2 (2010) 46–57
- D. Hue, S. Esquieu, Computational Drag Prediction of the DPW4 configuration using the far-field approach, *J. Aircraft* 48 (2011) 1658–1670
- E. Iuliano, D. Quagliarella, R.S. Donelli, I. Salah El Din, D. Arnal, Design of a supersonic natural laminar flow wing-body, *J. Aircraft* 48 (2011) 1147–1162
- G. Joubert, A. Le Pape, B. Heine, S. Huberson, Vortical interactions behind deployable vortex generator for airfoil static stall control, *AIAA J.* 51 (2013) 240–252
- J.-C. Jouhaud, M. Montagnac, L. Tourrette, A multi-grid adaptive mesh refinement strategy for 3D aerodynamic design, *Int. J. Numer. Methods Fluids* 47 (2005) 367–385
- J.-C. Jouhaud, P. Sagaut, B. Labeyrie, A kriging approach for CFD/Wind tunnel data comparison, *J. Fluid Eng.* 128 (2006) 847–855
- J.-C. Jouhaud, P. Sagaut, M. Montagnac, J. Laurenceau, A surrogate-model based multi-disciplinary shape optimization method with application to a 2d subsonic airfoil, *Comput. Fluids* 36 (2007) 520–529
- B. Landmann, M. Montagnac, A highly automated parallel Chimera method for overset grids based on the implicit hole cutting technique, *Int. J. Numer. Methods Fluids*, 66 (2011) 778–804
- J. Laurenceau, P. Sagaut, Building efficient response surfaces of aerodynamic functions with kriging and cokriging, *AIAA J.* 46 (2008) 498–507
- J. Laurenceau, M. Meaux, M. Montagnac, P. Sagaut, Comparison of gradient-based and gradient-enhanced response-surface-based optimizers, *AIAA J.* 48 (2010) 981–994
- C. Laurent, I. Mary, V. Gleize, A. Lerat, D. Arnal, DNS database of a transitional separation bubble on a flat plate and application to RANS modeling validation, *Comput. Fluids* 61 (2012) 21–30
- S. Lavagnoli, T. Yasa, G. Paniagua, L. Castillon, S. Duni, Aerodynamic analysis of an innovative low pressure vane placed in an s-shape duct, *J. Turbomach.* 134 (2012)
- G. Legras, N. Gourdain, I. Trebinjac, Numerical analysis of the tip leakage flow field in a transonic axial compressor with circumferential casing treatment, *J. Thermal Science* 19 (2010) 198–205
- G. Legras, I. Trebinjac, N. Gourdain, N. Ottavy, L. Castillon, A novel approach to evaluate the benefits of casing treatment in axial compressors, *Int. J. Rotating Machinery* DOI:10.1155/2012/975407 (2012)
- A. Le Pape, J. Lecanu, 3D Navier-Stokes computations of a stall regulated wind turbine, *Wind Energ.* 7 (2004) 309–324
- A. Le Pape, P. Beaumier, Numerical optimization of helicopter rotor aerodynamic performance in hover, *Aerosp. Sci. Technol.* 9 (2005) 191–201
- I. Lepot, M. Leborgne, R. Schnell, J. Yin, G. Delattre, F. Falissard, J. Talbotec, Aero-mechanical optimization of a contra-rotating open rotor and assessment of its aerodynamic and acoustic characteristics, *J. Power Energ.* 225 (2011) 850–863
- L.S. Lorente, J.M. Vega, A. Velazquez, Efficient computation of the POD manifold containing the information required to generate a multi-parameter aerodynamic database, *Aerosp. Sci. Technol.* 25 (2013) 152–160
- C. Marnignon, V. Couaillier, B. Courbet, Solution strategies for integration of semi-discretized flux equations in *elsA* and CEDRE, *Aerospace Lab 2* (2011)
- A. Marsan, I. Trébinjac, S. Coste, G. Leroy, Study and control of a radial vaned diffuser stall, *Int. J. Rotating Machinery* DOI:10.1155/2012/549048 (2012)
- J. Marty, B. Aupoix, Interaction of shrouded stator flow and main flow and its influence on performances of a three-stage high pressure compressor, *J. Power Energy* 226 (2012) 489–500
- Y. Mauffrey, G. Rahier, J. Prieur, Numerical investigation on blade/wake interaction noise generation, *J. Aircraft* 46 (2009) 1479–1486

- M. Méheut, D. Bailly, Drag-Breakdown methods from wake measurements, *AIAA J.* 46 (2008) 847–862
- M. Meunier, V. Brunet, High-lift devices performance enhancement using mechanical and air-jet vortex generators, *J. Aircraft* 45 (2008) 2049–2061
- M. Meunier, Simulation and optimization of flow control strategies for novel high-lift configurations, *AIAA J.* 47 (2009) 1145–1157
- B. Mialon et al., Validation of numerical prediction of dynamic derivatives, *Prog. Aerosp. Sci.* 47 (2011) 674–694
- F. Moens, J. Perraud, A. Séraudie, R. Houdeville, Transition measurement and prediction on a generic high-lift swept wing, *J. Aerosp. Eng.* 220 (2006) 589–603
- F. Moens, J. Perraud, A. Krumbein, T. Toulorge, P. Iannelli, P. Eliasson, A. Hanifi, Transition prediction and impact on a three-dimensional high-lift-wing configuration, *J. Aircraft* 45 (2008) 1751–1766
- B. Ortun, R. Boisard, I. Gonzalez-Martino, Assessment of propeller 1P loads predictions, *Int. J. Eng. Syst. Model. Simul.* 4 (2012) 36–46
- X. Ottavy, N. Courtiade, N. Gourdain, Experimental and computational methods for flow investigation in high-speed multistage compressor, *J. Propuls. Power* 28 (2012) 1141–1155
- G. Paniagua, T. Yasa, A. de la Loma, L. Castillon, T. Coton, Unsteady strong shocks interactions in a transonic turbine : experimental and numerical analysis, *J. Propuls. Power* 24 (2008)
- M. Pau, G. Paniagua, D. Delhayé, A. de la Loma, P. Ginibre, Aerothermal impact of stator-rim purge flow and rotor-platform film cooling on a transonic turbine stage, *J. Turbomach.* 132 (2010) 021006
- J. Perraud, F. Moens, A. Séraudie, Transition on a high lift swept wing in the European project EUROLIFT, *J. Aircraft* 41 (2004) 1183–1190
- J. Perraud, J. Cliquet, R. Houdeville, D. Arnal, F. Moens, Transport aircraft three-dimensional high-lift-wing numerical transition prediction, *J. Aircraft* 45 (2008) 1554–1563
- J. Peter, F. Drullion, Large stencil viscous flux linearization for the simulation of 3D compressible turbulent flows with backward-Euler schemes, *Comput. Fluids* 36 (2007) 1005–1027
- J. Peter, M. Marcelet, Comparison of surrogate models for turbomachinery design, *WSEAS Transactions on Fluid Mechanics* 1 (2007) 10–17
- J. Peter, M. Lazareff, V. Couaillier, Verification, validation and error estimation in CFD for compressible flows, *Int. J. Eng. Syst. Model. Simul.* 2 (2010) 75–87
- J. Peter, M. Nguyen-Dinh, P. Trontin, Goal oriented mesh adaptation using total derivative of aerodynamic functions with respect to mesh coordinates – With applications to Euler flows, *Comput. Fluids* 66 (2012) 194–214
- A. Placzek, D.M. Tran, R. Ohayon, A nonlinear POD-Galerkin reduced-order model for compressible flows taking into account rigid body motions, *Comput. Methods Appl. Mech. Eng.* 200 (2011) 3497–3514
- C. Polacsek, S. Burguburu, S. Redonnet, M. Terracol, Numerical simulations of fan interaction noise using a hybrid approach, *AIAA J.* 44 (2006) 1188–1196
- G. Reboul, C. Polacsek, Towards numerical simulation of fan broadband noise aft radiation from aero-engines, *AIAA J.* 28 (2010) 2038–2048
- S. Redonnet, Y. Druon, Computational aeroacoustics of aft fan noises characterizing a realistic co-axial engine, *AIAA J.* 50 (2012) 1029–1046
- F. Renac, Improvement of the recursive projection method for linear iterative scheme stabilization based on an approximate eigenvalue problem, *J. Comput. Phys.* 230 (2011) 5739–5752
- J. Reneaux, V. Brunet, S. Esquieu, M. Meunier, S. Mouton, Recent achievements in numerical simulation for aircraft power-plant configurations, *The Aeronautical Journal* 117 (2013) 1–17
- K. Richter, A. Le Pape, T. Knopp, M. Costes, V. Gleize, A.D. Gardner, Improved two-dimensional dynamic stall prediction with structured and hybrid numerical methods, *J. Amer. Helicopter Soc.* 56 (2011) 1–12
- N. Rochuon, I. Trébinjac, G. Billonnet, An extraction of the dominant rotor-stator interaction modes by the use of Proper Orthogonal Decomposition (POD), *J. Thermal Sciences* 15 (2006) 109–114
- N. Rochuon, I. Trébinjac, P. Kulisa, G. Billonnet, Assessment of jet-wake flow structures induced by three-dimensional hub wall contouring, *Int. Rev. Mech. Eng.* 2 (2008) 113–121
- A. Sachdeva, F. Leboeuf, Topological studies of Three-Dimensional Flows in a High Pressure Compressor Stator Blade Row without and with Boundary Layer Aspiration, *Chinese Journal of Aeronautics* 24 (2011) 541–549
- X. de Saint Victor, Estimation of the accuracy of numerical simulations using Richardson extrapolation and a Hessian technique, *Int. J. Eng. Syst. Model. Simul.* 2 (2010) 25–37
- X. de Saint Victor, Numerical simulations of unsteady separation bubbles over turbine blades, *Int. J. Fluid Mech. Res.* 39 (2012) 40–53
- S. Salvadori, F. Montomoli, F. Martelli, P. Adami, K.S. Chana, L. Castillon, Aerothermal study of the unsteady flow field in a transonic gas turbine with inlet temperature distortions, *J. Turbomach.* 133-031030 (2011) 1–13
- A. Séraudie, J. Perraud, F. Moens, Transition measurement and analysis on a swept wing in high lift configuration, *Aerosp. Sci. Technol.* 7 (2003) 569–576
- F. Sicot, G. Puigt, M. Montagnac, Block-Jacobi implicit algorithms for the time spectral method, *AIAA J.* 46 (2008) 3080–3089

- F. Sicot, T. Guedeney, G. Dufour, Time-domain harmonic balance method for aerodynamic and aeroelastic simulations of turbomachinery flows, *Int. J. Comput. Fluid Dyn.* DOI:10.1080/10618562.2012.740021 (2013)
- M. Thiery, E. Coustols, URANS computations of shock-induced oscillations over 2D rigid airfoils: influence of test section geometry, *Flow, Turbulence and Combustion* 74 (2005) 331–354
- M. Thiery, E. Coustols, Numerical prediction of shock-induced oscillations over a 2D airfoil: influence of turbulence modelling and test section walls, *Int. J. Heat Fluid Flow* 27 (2006) 661–670
- I. Trébinjac, P. Kulisa, N. Bulot, N. Rochuon, Effect of unsteadiness on the performance of a transonic centrifugal compressor stage, *J. Turbomach.* 131-041011 (2009) 1–9
- I. Trébinjac, N. Bulot, N. Buffaz, Analysis of the flow field in a transonic centrifugal compressor from choke to surge, *J. Power Energy* 225 (2011) 919–929
- M. Ueno, Y. Yamamoto, M. Yanagihara, M. Leplat, J. Oswald, Assessment of experimental and computational transonic base pressure using flight data, *J. Spacecraft Rockets* 44 (2007) 1241–1249
- P. Vass, T. Arts, Numerical investigation of high-pressure turbine blade tip flows: analysis of aerodynamics, *J. Power Energy* 225 (2011) 940–953
- J. Wild, J. Brézillon, O. Amoignon, J. Quest, F. Moens, D. Quagliarella, Advanced design by numerical methods and wind-tunnel verification within European high-lift program, *J. Aircraft* 46 (2009) 157–167
- W. Yamazaki, S. Mouton, G. Carrier, Geometry parameterization and computational mesh deformation by physics-based direct manipulation approaches, *AIAA J.* 48 (2010) 1817–1832
- [7] B. Aupoix, D. Arnal, H. Bézard, B. Chaouat, F. Chedevergne, S. Deck, V. Gleize, P. Grenard, E. Laroche, Transition and turbulence modeling, *Aerospace Lab 2* (2011)
- [8] H. Bézard, T. Daris, Calibrating the Length Scale Equation with an Explicit Algebraic Reynolds Stress Constitutive Relation, 6th Int. Symp. on Engineering Turbulence Modelling and Measurements, in Sardinia, W. Rodi and M. Mulas (eds.), Elsevier (2005) 77–86
- [9] S. Deck, Zonal-Detached Eddy Simulation of the Flow over a High-Lift Configuration, *AIAA J.* 43 (2005) 2372–2384
- [10] S. Deck, Recent improvements of the Zonal Detached Eddy Simulation (ZDES) formulation, *Theor. Comput. Fluid Dyn.* 26 (2012) 523–550
- [11] T. Renaud, M. Costes, S. Péron, Computation of GOAHEAD configuration with Chimera assembly, *Aerosp. Sci. Technol.* 19 (2012) 50–57
- [12] S. Péron, C. Benoit, Automatic off-body overset adaptive Cartesian mesh method based on an octree approach, *J. Comput. Phys.* 232 (2013) 153–173
- [13] G. Puigt, M. Gazaix, M. Montagnac, M.-C. Le Pape, M. de la Llave Plata, C. Marmignon, J.-F. Boussuge, V. Couaillier, Development of a new hybrid compressible solver inside the CFD *elsA* software, 20th AIAA CFD Conf., Honolulu, AIAA Paper 2011-3379, 2011
- [14] M. de la Llave Plata, V. Couaillier, M.-C. Le Pape, C. Marmignon, *elsA-Hybrid*: an all-in-one structured/unstructured solver for the simulation of internal and external flows. Application to turbomachinery, 4th EUCASS Conf., Saint-Petersburg, 2011
- [15] M. de la Llave Plata, V. Couaillier, C. Marmignon, M.-C. Le Pape, M. Gazaix, B. Cantaloube, Further developments in the multiblock hybrid CFD solver *elsA-H*, 40th AIAA ASM, Nashville, AIAA Paper 2012-1112, 2012
- [16] M. Errera, A. Dugeai, P. Girodroux-Lavigne, M. Pointot, Multi-physics coupling approaches for aerospace numerical simulations, *Aerospace Lab 2* (2011)
- [17] A. Dugeai, Y. Mauffrey, F. Sicot, Aeroelastic capabilities of the *elsA* solver for rotating machines applications, International Forum on Aeroelasticity and Structural Dynamics, Paris, 2011
- [18] J. Peter, G. Carrier, D. Bailly, P. Klotz, M. Marcelet, F. Renac, Local and global search methods for design in aeronautics, *Aerospace Lab 2* (2011)
- [19] J. Peter, R. Dwight, Numerical sensitivity analysis for aerodynamic optimization: A survey of approaches, *Comput. Fluids* 39 (2010) 373–391
- [20] A. Fosso-Pouangué, H. Deniau, F. Sicot, P. Sagaut, Curvilinear finite volume schemes using high order compact interpolation, *J. Comput. Phys.* 229 (2010) 5090–5122
- [21] A. Fosso-Pouangué, H. Deniau, N. Lamarque, T. Poinot, Comparison of outflow boundary conditions for subsonic aeroacoustic simulations, *Int. J. Numer. Methods Fluids* (2012)
- [22] G. Dufour, F. Sicot, G. Puigt, C. Liauzun, A. Dugeai, Oscillating-Flap Simulations with the Time-Spectral and Linearized Methods, *AIAA J.* 48 (2010) 788–797
- [23] F. Sicot, G. Dufour, N. Gourdain, A time-domain harmonic balance method for rotor/stator interactions, *J. Turbomach.* 134 (2012) 011001

References

- [24] Y. Colin, H. Deniau, J.-F. Boussuge, A robust low speed preconditioning formulation for viscous flow computations, *Comput. Fluids* 47 (2011) 1–15
- [25] N. Gourdain, L. Gicquel, M. Montagnac, O. Vermorel, M. Gazaix, G. Staffelbach, M. Garcia, J.-F. Boussuge, T. Poinso, High performance parallel computing of flows in complex geometries – part 1: methods, *Comput. Sci. Discovery* 2 (2009)
- [26] H. Tartousi, P. Kulisa, F. Leboeuf, G. Ngo Boum, A. Lefebvre, A. Yammine, Numerical investigation of a turbocharger centrifugal compressor: volute influence on the performance of the compressor, 9th European Turbomachinery Conf., Istanbul, 2011
- [27] M. Mesbah, J.-F. Thomas, F. Thirifay, R. Viguié, F. Durieu, V. Iliopoulou, O. De Vriendt, Investigation of compressor blade vibrations due to subharmonic aerodynamic excitations, 13th Int. Symp. on Unsteady Aerodynamics, Aeroacoustics and Aeroelasticity of Turbomachines (ISUAAAT), Tokyo, 2012
- [28] B. Michel, P. Cinnella, A. Lerat, Multiblock residual-based compact schemes for the computation of complex turbomachinery flows, *Int. J. Eng. Systems Model. Simul.* 3 (2011) 2–15
- [29] A. Lerat, P. Cinnella, B. Michel, F. Falissard, High-order residual-based compact schemes for aerodynamics and aeroacoustics, *Comput. Fluids* 61 (2012) 31–38
- [30] J. Babajee, T. Arts, Investigation of the laminar separation-induced transition with the γ - $Re\theta_t$ transition model on one very high-lift low-pressure turbine (T2) and one engine-like scale low-pressure turbine (TX) rotor blades at steady conditions and freestream turbulence, 47th 3AF Int. Symp. of Applied Aerodynamics, Paris, 2012
- [31] M. Stanciu, Y. Fendler, J.-M. Dorey, Unsteady stator-rotor interaction coupled with exhaust hood effect for last stage steam turbines, 9th European Turbomachinery Conf., Istanbul, 2011
- [32] S. Péron, C. Benoit, A Python module for Chimera assembly, 10th Overset Grid Symposium, <http://www.onera.fr/dsna/cassiopee/images/2010-09-OversetGridConnector.pdf>, NASA Ames, Moffett Field, 2010
- [33] S. Wallin, A.-V. Johansson, An explicit algebraic Reynolds stress model for incompressible and compressible turbulent flows, *J. Fluid Mech.* 403 (2000) 89–132
- [34] V. Brunet, Random flow generation technique for civil aircraft jet simulations with the ZDES approach, 4th Symp. on Hybrid RANS-LES methods, Beijing, 2011
- [35] A. Smirnov, S. Shi, I. Celik, Random Flow Generation Technique for Large Eddy Simulations and Particle Dynamics Modeling, *J. Fluid Eng.* 123 (2001) 359–371
- [36] S. Mouton, M. Lyonnet, Y. Le Sant, Prediction of the aerodynamic effect of model deformation during transonic wind tunnel tests, 47th 3AF Int. Symp. of Applied Aerodynamics, Paris, 2012